



Published in final edited form as:

Dev Dyn. 2009 October ; 238(10): 2522–2529. doi:10.1002/dvdy.22077.

Myosin-X is required for cranial neural crest cell migration in *Xenopus laevis*

Yoo-Seok Hwang, Ting Luo, Yanhua Xu, and Thomas D. Sargent*

Laboratory of Molecular Genetics, NICHD, NIH, Bldg 6B, Rm 412, 6 Center Drive, Bethesda MD, USA 20892

Abstract

Myosin-X (MyoX) belongs to a large family of unconventional, non-muscle, actin-dependent motor proteins. We show that MyoX is predominantly expressed in cranial neural crest (CNC) cells in embryos of *Xenopus laevis* and is required for head and jaw cartilage development. Knockdown of MyoX expression using antisense morpholino oligonucleotides resulted in retarded migration of CNC cells into the pharyngeal arches, leading to subsequent hypoplasia of cartilage and inhibited outgrowth of the CNC-derived trigeminal nerve. In vitro migration assays on fibronectin using explanted CNC cells showed significant inhibition of filopodia formation, cell attachment, spreading and migration, accompanied by disruption of the actin cytoskeleton. These data support the conclusion that MyoX has an essential function in CNC migration in the vertebrate embryo.

Keywords

MyoX; Myo10; Myosin-X; filopodia

Introduction

The neural crest (NC) originates at the boundary between the neural and non-neural ectoderm as the result of complex inductive interaction (Huang and Saint-Jeannet, 2004). As the neural folds meet and fuse, NC cells undergo a classical epithelial-mesenchymal transition, delaminate from the neuroepithelium and subsequently migrate throughout the body, finally differentiating into a large number of distinct cell and tissue types (Bronner-Fraser, 1993; Le Douarin, 1999). In the anterior region of the embryo, the cranial NC (CNC) cells originating from the presumptive hindbrain migrate in coherent streams into the ventrally located pharyngeal pouches, giving rise to the pharyngeal arches that differentiate into jaw cartilage and bone, as well as some other structures including portions of the cranial ganglia and nerves (Schlosser, 2006). One key transcription factor is TFAP2a, one of a five-member subfamily of transcriptional activator (Eckert et al., 2005). TFAP2a has been shown by loss of function experiments to be essential for the maintenance and subsequent differentiation of CNC in vertebrates (Schorle et al., 1996; Zhang et al., 1996; Knight et al., 2003; Luo et al., 2003). In neuralized *Xenopus* ectoderm, ectopic expression of TFAP2a resulted in repression of neural genes and activation of the NC transcriptional program (Luo et al., 2003). We have used this as an assay for identification of TFAP2a target genes expressed in NC (Luo et al., 2005). Among the most highly induced genes discovered in this screen was the unconventional myosin, MyoX.

*Corresponding author Tel. 301 496 0369 Fax. 301 496 0243 tsargent@nih.gov.

MyoX is one of approximately a dozen different classes of myosin expressed in vertebrates (Berg et al., 2001) characterized by a N-terminal actin-dependent motor domain and variable C-terminal tails with binding sites for a number of cytoskeletal components, plasma membrane, signaling molecules and other factors (Sousa and Cheney, 2005). The head of MyoX binds directly to actin filaments and generates intracellular movement (Homma et al., 2001). The MyoX tail includes a FERM domain (band 4.1, ezrin, radixin and moesin) which interacts with some beta integrins, and is important in cell attachment (Zhang et al., 2004). In cultured cells, MyoX has been shown to be both necessary and sufficient for the formation of filopodia (Bohil et al., 2006). MyoX has additional functions in phagocytosis (Cox et al., 2002), intercellular adhesion (Yonezawa et al., 2003) and endocytosis (Tacon et al., 2004). However, the functions of MyoX in intact organisms have not been thoroughly studied. To investigate this in vertebrate development, we have used loss-of-function analysis in *Xenopus* embryos. We have found that MyoX is strongly expressed in the CNC, and that the zygotic expression of MyoX is required for CNC cell migration from the hindbrain to the pharyngeal arches. Thus MyoX has been established as an essential component of craniofacial development in the vertebrate embryo.

Results

MyoX is predominantly expressed in cranial neural crest (CNC)

MyoX is vertebrate-specific and has been shown to be expressed in many cells and tissues (Berg et al., 2000). MyoX mRNA is present maternally, and at all stages of development in *Xenopus* (Fig. 1A). MyoX RNA is not uniformly expressed spatially, however, and is most abundant in cranial and trunk NC at neurula stages (Fig. 1B-D). MyoX RNA is also abundant in paraxial mesoderm and the anterior neural plate (Fig. 1B). By tailbud stage (st. 21) MyoX expression persists in migratory CNC cells, then declines following the completion of NC migration to form the pharyngeal arches (Fig. 1E,F). By stage 33/34 expression in cranial ganglia is visible while pharyngeal arch expression becomes undetectable (Fig. 1G, H).

MyoX knockdown results in head cartilage hypoplasia

Maternal MyoX has been shown to have critical functions in both meiosis and mitosis in *Xenopus* (Weber et al., 2004; Woolner et al., 2008). In order to test if MyoX is required for CNC development, we used antisense morpholino oligonucleotides (MOs) to specifically inhibit zygotic MyoX pre-mRNA splicing. This strategy circumvents inhibition of the essential maternal MyoX expression, allowing embryonic survival beyond early cleavage stages. Two MOs were designed (named MO1 and MO2), and both were shown to specifically and substantially block processing of MyoX RNA (see Supporting Information, Fig.S1 online). Injection of either MO resulted in significant reductions in head size, (100 %, n=255 for MO1; 93%, n=231 for MO2; Fig. 2A). Alcian blue staining revealed that all head cartilage elements were present in morphants, but were dramatically reduced in size (Fig. 2B).

To quantify this defect, we measured tadpole head width following injection of MO or water as control. As shown in Fig.2C, the average width of controls was 1.60 mm (blue dotted line), whereas that of MO1 or MO2 was 1.13 mm. We also performed the MO co-injection along with increasing doses of GFP-fused MyoX mRNA in an attempt to rescue the morphant phenotype and rule out nonspecific MO effects. At the 6ng dose of co-injected GFP-MyoX RNA, the narrow head phenotype was rescued significantly, especially for MO2, which approached control levels. This strongly supports the conclusion that MyoX is required for head cartilage development.

The morphant phenotype is due to a cell-autonomous defect in neural crest migration

During *Xenopus* head development, CNC cells migrate from hindbrain in a segmental manner to contribute to the skeletal cartilage (Sadaghiani and Thiebaud, 1987). Induction of NC occurs during gastrulation as the result of complex interactions involving neural ectoderm and adjacent epidermis and paraxial mesoderm (Bonstein et al., 1998). As shown in Figure 1, MyoX is expressed at high levels in the latter tissue, raising the possibility that the observed CNC defects might be the result of abnormal NC induction due to defects in adjacent tissues, such as mesoderm or epidermis. This was investigated by in situ hybridization with tissue-specific probes at early embryonic stages. No significant changes were observed in MyoX knockdown embryos (Fig. 3A), including *snail2* (also called *slug*), which is an early marker for NC induction (Mayor et al., 1995). In addition, gastrulation proceeded normally in these embryos (data not shown). Therefore the observed defects in craniofacial development must be the result of abnormalities in subsequent migration or defective terminal differentiation of NC cells. This interpretation was supported by in situ hybridization with *Sox9* (Spokony et al., 2002), and *Sox10* (Aoki et al., 2003) probes at tailbud stages, both of which clearly demarcate NC. Both markers revealed retarded migration of cranial NC cells on the MO-knockdown side (Fig. 3B). The migration defect was not accompanied by apoptotic cell death: TUNEL assays from early neurula to st. 24 tailbud did not show significant increases in signal on the MO-knockdown side (Fig. S2). The morphant phenotype was not limited to cartilage, but also affects other CNC derivatives in the head. As shown in Figure 3C, MyoX knockdown also inhibited trigeminal nerve outgrowth, indicated by *Sox10* expression at st. 32 (Cheng et al., 2000; De Bellard et al., 2002).

The transplantation assay has been well established to study the migratory behavior of CNC cells in *Xenopus* (Borchers et al., 2000). To test for cell autonomy of the MyoX knockdown phenotype, transplantation experiments were carried out. Premigratory CNC, with overlying ectoderm, was isolated from fluorescently-labeled MyoX knockdown and control embryos and transplanted into unlabeled host embryos. To lessen the possibility of MyoX knockdown in adjacent tissues, which might affect the CNC phenotype, the MO in these experiments was targeted to the appropriate blastomeres at the 16–32 cell stage. This strategy would not prevent possible knockdown of MyoX activity in adjacent epidermis, but the MyoX RNA expression level is extremely low in epidermis (Fig. 1C), and this tissue developed normally in the knockdown embryos (Fig 3A). Therefore we believe a role for epidermal MyoX in the CNC phenotype is unlikely. As shown in Figure 4, control transplants migrated normally and formed essentially complete craniofacial structures by St. 45. However, MO2 knockdown cells exhibited delayed migration and significant reduction in cranial cartilage on the grafted side, similar to the previous experiments. These results support the conclusion that MyoX functions in NC migration, and does so in a cell-autonomous manner.

MyoX knockdown results in defects in cell attachment, spreading and migration in vitro

Xenopus laevis CNC cells migrate efficiently in vitro on a fibronectin substrate, requiring integrin α 5 β 1 as the primary receptor complex (Alfandari et al., 2003). To test the ability of MyoX knockdown cells to migrate in vitro, CNC explants were dissected from stage 17 embryos injected with either control MO or MO2 and plated on plastic dishes coated with fibronectin. Migration was monitored over a 20-hour period. As shown in Fig. 5A and Movie S1, control NC cells migrated extensively from the explant, often maintaining coherent streams that likely correspond to pharyngeal arch populations in vivo. However, the majority of CNC cells from MO2-injected embryos failed to migrate. Furthermore, knockdown cells exhibited a rounded morphology lacking filopodia (Fig. 5D, E, Movie S2). These cells attached only weakly to the substrate and, unlike control NC cells, could be easily stripped from the slide by gentle pipetting or agitation (data not shown). This

phenotype was more severe than what was observed in the intact embryo. However, since these defects were significantly rescued by co-injection of MyoX RNA, nonspecific artifacts can be ruled out, supporting the conclusion that MyoX is required for CNC cell migration, and probably for substrate adhesion as well, at least in vitro (Fig. 5C, D, E and Movie S3).

Discussion

MyoX is a ubiquitous, essential protein required for basic cellular processes including mitosis, and meiosis (Weber et al., 2004; Bohil et al., 2006; Woolner et al., 2008). In addition to these activities, the MyoX gene has tissue-specific functions, including cargo transport in neurons and endothelial cells (Pi et al., 2007; Zhu et al., 2007). In this report, we have shown that MyoX is expressed at relatively high levels in the CNC, and that this expression is critical for the migration and subsequent differentiation of CNC into derivative tissues such as cranial cartilage and ganglia.

The critical function of MyoX in filopodial formation has been well-established (Bohil et al., 2006). At the leading edge of migratory cells filopodia can act as sensors to explore the local environment for directional cues. Filopodia also provide initial attachment to the substrate (Partridge and Marcantonio, 2006) which, when stabilized, provides the traction enabling the cell to move forward (Heidemann et al., 1990; Bridgman et al., 2001). Filopodial formation is dependent on MyoX and this is likely to be an essential component of NC cell migration. One possible explanation for the craniofacial phenotype caused by knockdown of MyoX is that reduced CNC cell migration resulted in a deficit of pharyngeal arch mesenchyme. Another alternative is suggested by our observation that MyoX knockdown CNC cells were unable to attach to fibronectin in vitro. If a similar defect occurs in vivo in the MyoX knockdown CNC cells, this might result in signaling defects. For example, in mammalian NC cells association of integrin with extracellular matrix components has been shown to activate multiple signal transduction responses (Desban et al., 2006). Since NC cells acquire much of their differentiation potential by inductive interactions during and after migration (Le Douarin et al., 2004), it is possible that MyoX knockdown CNC cells are unable to receive such inductive cues, leading to a failure to differentiate properly. On the other hand, while slowed, CNC migration in MyoX knockdown embryos did not appear to be mis-directed; cells derived from different regions from the hindbrain targeted the appropriate pharyngeal arches, and other destinations in the head. Furthermore there was little if any increase in apoptosis resulting from MyoX knockdown, suggesting that at least some signaling between CNC and adjacent cells was intact. Nevertheless we can not rule out the possibility that separate signals could support migration targeting versus differentiation cues. Conceivably, the role of MyoX in CNC could be even more complex. In addition to integrins, other cargoes for MyoX have been identified, such as DCC (Zhu et al., 2007), VASP (Tokuo and Ikebe, 2004), and the receptor for BMP6 (Pi et al., 2007). Defects in transport of such molecules could result in abnormal CNC migration or differentiation.

Loss of maternal MyoX results in disruption of cleavage and embryonic lethality (Woolner et al., 2008); YS Hwang, unpublished). Based on the absence of apoptosis in the knockdown embryos (Fig. S2) and the absence of alterations in early gene expression in NC or other cell types, we speculate that in contrast to maternal MyoX, the zygotic expression of this gene is not required for normal cell division. One trivial alternative could be that the knockdown of MyoX in our experiments was incomplete, providing enough residual protein for normal spindle formation. It is also conceivable that another member of the myosin gene family could provide some redundancy for essential MyoX functions, although there is no evidence to support this notion. A more interesting possibility is that the requirement for maternal MyoX in mitosis is specific to the rapid cleavage cycles during blastula stages in *Xenopus*

(Newport and Kirschner, 1984) and is dispensable in more slowly dividing cells. Additional loss-of-function experiments will be required to resolve this question.

MyoX expression is also elevated in other tissues in early development, such as trunk NC, paraxial mesoderm forebrain and presumptive gut endoderm (not shown). While we have not examined derivatives of these tissues in detail, they did not exhibit any obvious defect except for the gut, which exhibited defective coiling (not shown). Forebrain abnormalities have not been ruled out, but would be difficult to discriminate from secondary effects of the cranial bone deficiency. The most likely interpretation is that CNC cells have an elevated sensitivity to loss of MyoX compared to the other highly-expressing tissues. Presumably this differential sensitivity reflects some special property of CNC, such as the highly migratory nature of this cell type, necessitating rapid and dynamic transport of adhesion proteins including integrins to filopodial tips where cell-substrate and cell-cell contacts are promoted. The observed defect in projection of cranial nerve V could also be an indirect result of delayed NC migration. However, an alternative hypothesis is that MyoX is required for outgrowth of the cranial nerve per se, similar to what has been reported for neurons from both chick and mouse embryos in which MyoX function has been inhibited (Zhu et al., 2007).

Compared to in vivo migration defects, the phenotype of isolated MyoX knockdown CNC explants on fibronectin substrate was very severe. Not only was migration virtually eliminated, but cell-substrate adhesion was severely reduced, and cytoskeletal organization was disrupted as well. One possibility is that in vivo, other extracellular matrix components in addition to fibronectin might contribute to providing the substrate for CNC migration. In *Xenopus*, integrin α 5 β 1 and α 3 β 1 are present on the CNC cell surface (Alfandari et al., 2003). Since integrin α 3 β 1 binding to laminin 5 is involved in cell migration and cell invasion (Giannelli et al., 2002), it is possible this type of laminin also important for CNC migration in vivo. It is also possible that the artificial environment provided by purified fibronectin on glass or plastic surfaces induces additional stress to CNC cells, or lacks signals that are required for robust migration in vivo.

We have shown that MyoX has been recruited to serve as an essential component of CNC cell adhesion and migration. NC cells are among the most migratory in development, needing to rapidly travel from their origin in the neural folds throughout the entire body, following defined paths and undergoing complex terminal differentiation depending on signals received en route. Compared to the initial induction of NC, such later differentiation signals are very poorly understood. Understanding the role of integrin-dependent signaling in CNC, identifying other proteins in addition to integrin β 1 with which MyoX interacts in CNC, and further elucidating the importance of MyoX-dependent filopodial formation in CNC development will be important areas for future research.

Experimental Procedures

Plasmid constructs

Myc-MyoX was generated by transferring a PCR-amplified MyoX coding fragment into a modified pCS2+ vector that adds a single myc epitope at the amino-terminus. GFP-MyoX was a gift from William M. Bement (Weber et al., 2004).

Morpholino Oligonucleotides (MOs)

Based on *Xenopus tropicalis* genome information (Ensembl Gene ID: ENSXETG00000007165), five short intronic regions within the MyoX motor domain were selected as candidate sites for splice-inhibitory morpholino design. Primers (sequences available upon request) flanking these introns in the *X. laevis* MyoX mRNA sequence were

used to amplify *X. laevis* genomic DNA fragments, which were cloned into pGEM-T (Promega) and sequenced. One splice acceptor site (intron 3, MO1) and one splice donor site (intron9, MO2) were chosen as targets and were synthesized by Gene tools, LLC. MO1: TCC CCA CTG TAA CGG GAA GCA TGG T. MO2: GGT GCT GCT GCA TTA CCT GCT TTG C. MO doses were determined by titration using cranial morphology and RT-PCR to evaluate effectiveness; a minimum of 60 ng/embryo of each MO was required.

Embryo manipulation, in situ hybridization, Alcian Blue staining, whole-mount TUNEL and immunofluorescence

Xenopus embryos were obtained and staged according to standard procedures (Sive et al., 2000). For RT-PCR, total RNA was extracted from embryos using TRIzol (Invitrogen), and synthesis of oligo-dT primed cDNA was performed with Superscript II reverse transcriptase (Invitrogen) according to manufacturer's instructions. For the MyoX in situ probe a fragment corresponding to the FERM domain and 3'UTR was amplified by PCR from the NIBB clone XL085p13 and cloned in pBluescript SK (-). Other antisense probes for Snail2 (Mayor et al., 1995), Sox2 (Mizuseki et al., 1998), Sox9 (Spokony et al., 2002), Sox10 (Aoki et al., 2003), MyoD (Frank and Harland, 1991), XK81 (Jonas et al., 1985) were labeled with digoxigenin, and whole-mount in situ hybridization procedures were performed according to standard methods (Harland, 1991). Alcian Blue cartilage staining was performed as described (Pasqualetti et al., 2000). TUNEL staining was previously described (Huang et al., 2007) using 1X TdT buffer (TdT recombinant; Invitrogen; 10533-065), 1 μ M digoxigenin – dUTP (Roche; 11-093-088-910) and anti-digoxigenin AP antibody (Roche; 11-093-274-910).

CNC transplantation and in vitro CNC migration assays

CNC transplantation (Borchers et al., 2000) and in vitro migration assays (DeSimone, 2005) were performed as previously described. Images were captured at 8m 40s intervals for 26 hr using an automated stage-aided Zeiss Duoscan confocal microscope (10x objective). The area of the migrated cell mass was measured using the Metamorph program. Data sets from two separate experiments were combined to generate plots and to perform ANOVA (analysis of variance).

Phalloidin staining of migrated CNC cells

CNC explants were cultured for 20 hr at 19°C in a plastic chamber slide, then fixed by gently adding an equal volume of 2XFG fix (1X FG: 3.7% formaldehyde, 0.25% glutaraldehyde, 0.2% TritonX-100 in Pipes buffer; (Gard et al., 1997), after 5 min samples were washed 3 times for 30 min in 1XPBS, 0.1% Tween20, treated with rhodamine-labeled phalloidin (Invitrogen Molecular Probes, Cat#R415, 5u/ml) at RT for 2 hr, then washed 3 times for 30 min in 1xPBS. Slides were mounted in VECTASHIELD with DAPI (H-1200), and air-dried in dark overnight. Images were obtained using a Zeiss Axioplan fluorescent microscope.

Statistical analysis

To estimate the significance of differential migration and cell rounding, we carried out analysis of variance (ANOVA; Fig.5C, E) with Dunnett T3 Post Hoc Tests and Duncan's homogenous subset grouping (Fig. S4). Data from the four experimental groups representing differential cellular level of MyoX underwent One-way ANOVA analysis. The effects of four different conditions on CNC cell migration and attachment were highly significant (sig. < 0.000~) showing that the MO2 injected group was the most affected and significantly different from the other three groups. (Duncan's Homogenous subset grouping; Fig. S4).

Supplementary Material

Refer to Web version on PubMed Central for supplementary material.

Acknowledgments

We thank Dr. William Bement for providing the GFP-MyoX construct. We are also grateful to V. Schram (Microscopy and Imaging Core, NICHD) for valuable assistance with confocal microscopy, and Dr. Sheran Law for discussions. This work was supported by the Intramural Research Program of the National Institute of Child Health and Human Development, NIH.

References

- Alfandari D, Cousin H, Gaultier A, Hoffstrom BG, DeSimone DW. Integrin alpha5beta1 supports the migration of *Xenopus* cranial neural crest on fibronectin. *Dev Biol.* 2003; 260:449–464. [PubMed: 12921745]
- Aoki Y, Saint-Germain N, Gyda M, Magner-Fink E, Lee YH, Credidio C, Saint-Jeannet JP. Sox10 regulates the development of neural crest-derived melanocytes in *Xenopus*. *Dev Biol.* 2003; 259:19–33. [PubMed: 12812785]
- Berg JS, Derfler BH, Pennisi CM, Corey DP, Cheney RE. Myosin-X, a novel myosin with pleckstrin homology domains, associates with regions of dynamic actin. *J Cell Sci.* 2000; 113(Pt 19):3439–3451. [PubMed: 10984435]
- Berg JS, Powell BC, Cheney RE. A millennial myosin census. *Mol Biol Cell.* 2001; 12:780–794. [PubMed: 11294886]
- Bohil AB, Robertson BW, Cheney RE. Myosin-X is a molecular motor that functions in filopodia formation. *Proc Natl Acad Sci U S A.* 2006; 103:12411–12416. [PubMed: 16894163]
- Bonstein L, Elias S, Frank D. Paraxial-fated mesoderm is required for neural crest induction in *Xenopus* embryos. *Dev Biol.* 1998; 193:156–168. [PubMed: 9473321]
- Borchers A, Epperlein HH, Wedlich D. An assay system to study migratory behavior of cranial neural crest cells in *Xenopus*. *Dev Genes Evol.* 2000; 210:217–222. [PubMed: 11180825]
- Bridgman PC, Dave S, Asnes CF, Tullio AN, Adelstein RS. Myosin IIB is required for growth cone motility. *J Neurosci.* 2001; 21:6159–6169. [PubMed: 11487639]
- Bronner-Fraser M. Neural crest cell migration in the developing embryo. *Trends Cell Biol.* 1993; 3:392–397. [PubMed: 14731657]
- Cheng Y, Cheung M, Abu-Elmagd MM, Orme A, Scotting PJ. Chick sox10, a transcription factor expressed in both early neural crest cells and central nervous system. *Brain Res Dev Brain Res.* 2000; 121:233–241.
- Cox D, Berg JS, Cammer M, Chingewundoh JO, Dale BM, Cheney RE, Greenberg S. Myosin X is a downstream effector of PI(3)K during phagocytosis. *Nat Cell Biol.* 2002; 4:469–477. [PubMed: 12055636]
- De Bellard ME, Ching W, Gossler A, Bronner-Fraser M. Disruption of segmental neural crest migration and ephrin expression in delta-1 null mice. *Dev Biol.* 2002; 249:121–130. [PubMed: 12217323]
- Desban N, Lissitzky JC, Rousselle P, Duband JL. alpha1beta1-integrin engagement to distinct laminin-1 domains orchestrates spreading, migration and survival of neural crest cells through independent signaling pathways. *J Cell Sci.* 2006; 119:3206–3218. [PubMed: 16847051]
- DeSimone, DW.; Davidson, L.; Marsden, M.; Alfandari, D. The *Xenopus* embryo as a model system for studies of cell migration. In: Guan, J-L., editor. *Cell Migration: Developmental Methods and Protocols*. Totowa, NJ: Humana Press; 2005.
- Detrick RJ, Dickey D, Kintner CR. The effects of N-cadherin misexpression on morphogenesis in *Xenopus* embryos. *Neuron.* 1990; 4:493–506. [PubMed: 2322458]
- Eckert D, Buhl S, Weber S, Jager R, Schorle H. The AP-2 family of transcription factors. *Genome Biol.* 2005; 6:246. [PubMed: 16420676]
- Frank D, Harland RM. Transient expression of XMyoD in non-somitic mesoderm of *Xenopus* gastrulae. *Development.* 1991; 113:1387–1393. [PubMed: 1667381]

- Gard DL, Cha BJ, King E. The organization and animal-vegetal asymmetry of cytokeratin filaments in stage VI *Xenopus* oocytes is dependent upon F-actin and microtubules. *Dev Biol.* 1997; 184:95–114. [PubMed: 9142987]
- Giannelli G, Astigiano S, Antonaci S, Morini M, Barbieri O, Noonan DM, Albin A. Role of the alpha3beta1 and alpha6beta4 integrins in tumor invasion. *Clin Exp Metastasis.* 2002; 19:217–223. [PubMed: 12067202]
- Harland RM. In situ hybridization: an improved whole-mount method for *Xenopus* embryos. *Methods Cell Biol.* 1991; 36:685–695. [PubMed: 1811161]
- Heidemann SR, Lamoureux P, Buxbaum RE. Growth cone behavior and production of traction force. *J Cell Biol.* 1990; 111:1949–1957. [PubMed: 2229183]
- Homma K, Saito J, Ikebe R, Ikebe M. Motor function and regulation of myosin X. *J Biol Chem.* 2001; 276:34348–34354. [PubMed: 11457842]
- Honore E, Hemmati-Brivanlou A. In vivo evidence for trigeminal nerve guidance by the cement gland in *Xenopus*. *Dev Biol.* 1996; 178:363–374. [PubMed: 8812135]
- Huang JK, Dorey K, Ishibashi S, Amaya E. BDNF promotes target innervation of *Xenopus* mandibular trigeminal axons in vivo. *BMC Dev Biol.* 2007; 7:59. [PubMed: 17540021]
- Huang X, Saint-Jeannet JP. Induction of the neural crest and the opportunities of life on the edge. *Dev Biol.* 2004; 275:1–11. [PubMed: 15464568]
- Jonas E, Sargent TD, Dawid IB. Epidermal keratin gene expressed in embryos of *Xenopus laevis*. *Proc Natl Acad Sci U S A.* 1985; 82:5413–5417. [PubMed: 2410923]
- Knight RD, Nair S, Nelson SS, Afshar A, Javidan Y, Geisler R, Rauch GJ, Schilling TF. *lockjaw* encodes a zebrafish *tfap2a* required for early neural crest development. *Development.* 2003; 130:5755–5768. [PubMed: 14534133]
- Le Douarin NM, Creuzet S, Couly G, Dupin E. Neural crest cell plasticity and its limits. *Development.* 2004; 131:4637–4650. [PubMed: 15358668]
- Le Douarin, NM.; Kalcheim, C. *The Neural Crest.* Cambridge, U.K: Cambridge Univ. Press; 1999.
- Luo T, Lee YH, Saint-Jeannet JP, Sargent TD. Induction of neural crest in *Xenopus* by transcription factor AP2alpha. *Proc Natl Acad Sci U S A.* 2003; 100:532–537. [PubMed: 12511599]
- Luo T, Zhang Y, Khadka D, Rangarajan J, Cho KW, Sargent TD. Regulatory targets for transcription factor AP2 in *Xenopus* embryos. *Dev Growth Differ.* 2005; 47:403–413. [PubMed: 16109038]
- Mayor R, Morgan R, Sargent MG. Induction of the prospective neural crest of *Xenopus*. *Development.* 1995; 121:767–777. [PubMed: 7720581]
- Mizuseki K, Kishi M, Matsui M, Nakanishi S, Sasai Y. *Xenopus* *Zic*-related-1 and *Sox-2*, two factors induced by chordin, have distinct activities in the initiation of neural induction. *Development.* 1998; 125:579–587. [PubMed: 9435279]
- Nagata S, Yamada Y, Saito R, Fujita N. Overexpression of receptor-type protein tyrosine phosphatase beta causes abnormal development of the cranial nerve in *Xenopus* embryos. *Neurosci Lett.* 2003; 349:175–178. [PubMed: 12951197]
- Newport JW, Kirschner MW. Regulation of the cell cycle during early *Xenopus* development. *Cell.* 1984; 37:731–742. [PubMed: 6378387]
- Partridge MA, Marcantonio EE. Initiation of attachment and generation of mature focal adhesions by integrin-containing filopodia in cell spreading. *Mol Biol Cell.* 2006; 17:4237–4248. [PubMed: 16855018]
- Pasqualetti M, Ori M, Nardi I, Rijli FM. Ectopic *Hoxa2* induction after neural crest migration results in homeosis of jaw elements in *Xenopus*. *Development.* 2000; 127:5367–5378. [PubMed: 11076758]
- Pi X, Ren R, Kelley R, Zhang C, Moser M, Bohil AB, Divito M, Cheney RE, Patterson C. Sequential roles for myosin-X in BMP6-dependent filopodial extension, migration, and activation of BMP receptors. *J Cell Biol.* 2007; 179:1569–1582. [PubMed: 18158328]
- Sadaghiani B, Thiebaud CH. Neural crest development in the *Xenopus laevis* embryo, studied by interspecific transplantation and scanning electron microscopy. *Dev Biol.* 1987; 124:91–110. [PubMed: 3666314]
- Schlusser G. Induction and specification of cranial placodes. *Dev Biol.* 2006; 294:303–351. [PubMed: 16677629]

- Schorle H, Meier P, Buchert M, Jaenisch R, Mitchell PJ. Transcription factor AP-2 essential for cranial closure and craniofacial development. *Nature*. 1996; 381:235–238. [PubMed: 8622765]
- Sive, HL.; Grainger, RM.; Harland, RM. Early development of *Xenopus laevis* : a laboratory manual. Vol. ix. Cold Spring Harbor, N.Y: Cold Spring Harbor Laboratory Press; 2000. p. 338[337] p. of plates pp
- Sousa AD, Cheney RE. Myosin-X: a molecular motor at the cell's fingertips. *Trends Cell Biol*. 2005; 15:533–539. [PubMed: 16140532]
- Spokony RF, Aoki Y, Saint-Germain N, Magner-Fink E, Saint-Jeannet JP. The transcription factor Sox9 is required for cranial neural crest development in *Xenopus*. *Development*. 2002; 129:421–432. [PubMed: 11807034]
- Tacon D, Knight PJ, Peckham M. Imaging myosin 10 in cells. *Biochem Soc Trans*. 2004; 32:689–693. [PubMed: 15493989]
- Tokuo H, Ikebe M. Myosin X transports Mena/VASP to the tip of filopodia. *Biochem Biophys Res Commun*. 2004; 319:214–220. [PubMed: 15158464]
- Weber KL, Sokac AM, Berg JS, Cheney RE, Bement WM. A microtubule-binding myosin required for nuclear anchoring and spindle assembly. *Nature*. 2004; 431:325–329. [PubMed: 15372037]
- Woolner S, O'Brien LL, Wiese C, Bement WM. Myosin-10 and actin filaments are essential for mitotic spindle function. *J Cell Biol*. 2008; 182:77–88. [PubMed: 18606852]
- Yonezawa S, Yoshizaki N, Sano M, Hanai A, Masaki S, Takizawa T, Kageyama T, Moriyama A. Possible involvement of myosin-X in intercellular adhesion: importance of serial pleckstrin homology regions for intracellular localization. *Dev Growth Differ*. 2003; 45:175–185. [PubMed: 12752505]
- Zhang H, Berg JS, Li Z, Wang Y, Lang P, Sousa AD, Bhaskar A, Cheney RE, Stromblad S. Myosin-X provides a motor-based link between integrins and the cytoskeleton. *Nat Cell Biol*. 2004; 6:523–531. [PubMed: 15156152]
- Zhang J, Hagopian-Donaldson S, Serbedzija G, Elsemore J, Plehn-Dujowich D, McMahon AP, Flavell RA, Williams T. Neural tube, skeletal and body wall defects in mice lacking transcription factor AP-2. *Nature*. 1996; 381:238–241. [PubMed: 8622766]
- Zhu XJ, Wang CZ, Dai PG, Xie Y, Song NN, Liu Y, Du QS, Mei L, Ding YQ, Xiong WC. Myosin X regulates netrin receptors and functions in axonal pathfinding. *Nat Cell Biol*. 2007; 9:184–192. [PubMed: 17237772]

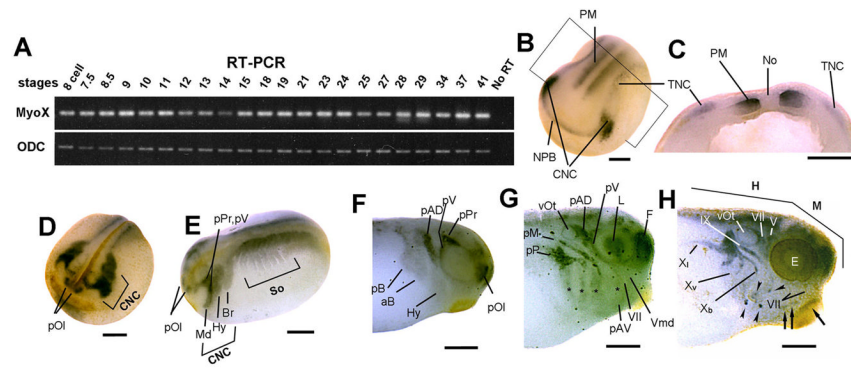


Figure 1. Spatial and temporal expression of MyoX in Xenopus

(A) RT-PCR analysis. MyoX mRNA was detected at all embryonic stages. (B-H) Whole mount ISH. Stages are: St. 16 neurula (B,C), St. 19 neurula (D), St. 21 tailbud (E), St. 24 tailbud (F), St. 33 tadpole (G) and St. 38 tadpole (H). Panel (C) is a transverse section of the embryo in panel (B). Early MyoX expression is most abundant in cranial neural crest (CNC), trunk neural crest (TNC), paraxial mesoderm (PM) and the anterior neural plate border (NPB). Later, strong expression is visible in placodes (D-G). In the tadpole, MyoX signal is elevated in cranial nerve V~X, termini of nerve IX, X (arrow heads) and three termini of nerve VII (arrows, also see Fig. S3), and in epibranchial placodes (asterisks, G). Abbreviations: aB: anterior branchial arch, Br: branchial arch, F: forebrain H: hindbrain, Hy: hyoid arch, IX: glossopharyngeal nerve, L: lens placode, M: midbrain, Md: mandibular arch, No: notochord, So: somites, pAD: anterodorsal placode, pAV: anteroventral placode, pB: posterior branchial arch, pM: middle lateral line placode, pOI: olfactory placode, pP: posterior lateral line placode, pPr: profundal placode, pV: trigeminal placode, V: trigeminal nerve, Vmd: mandibular branch of trigeminal nerve, VII: facial nerve, vOt: otic vesicle, X_b: branchial branch - cranial nerve X, X_i: lateral branch - cranial nerve X, X_v: visceral branch - cranial nerve X.

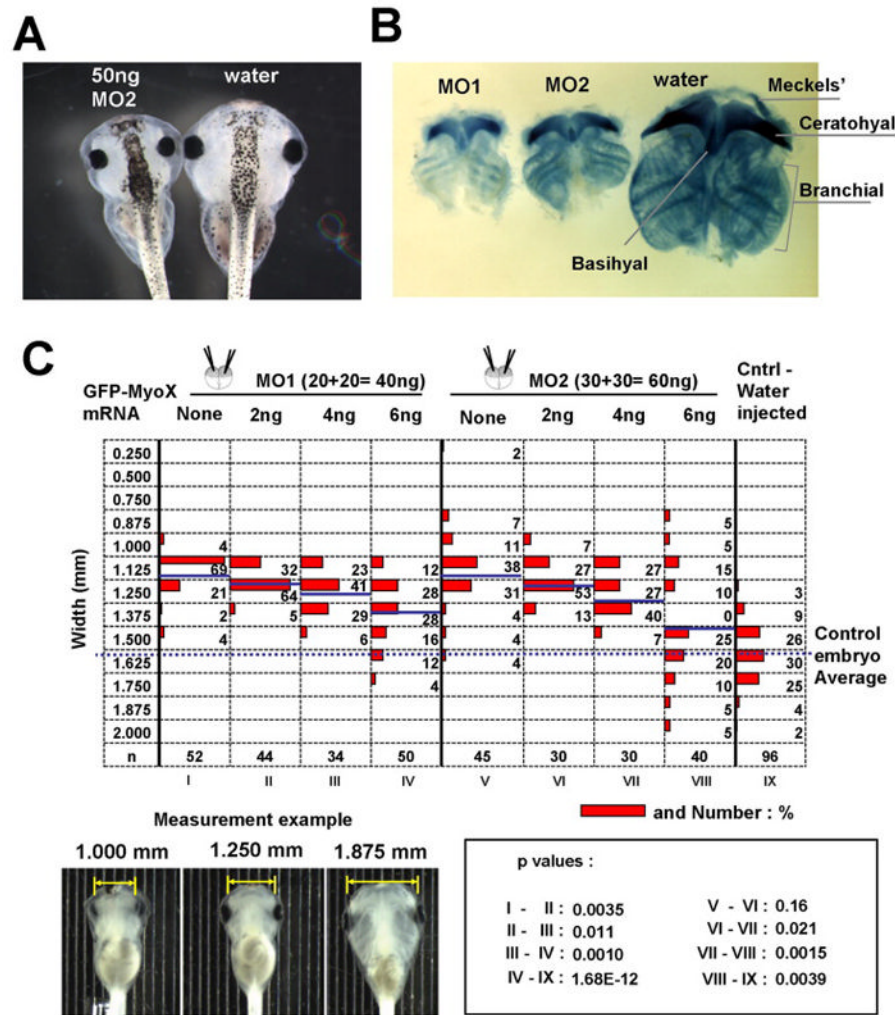


Figure 2. Head cartilage defects in MyoX knockdown embryos

(A) MyoX MOs that was injected bi-laterally resulted in cranial cartilage defects and reduced head size at St. 45. Left; MO2 50ng. Right, water control. (B) Alcian Blue staining revealed all elements of cranial cartilage present but reduced in size by both MOs (MO1:40ng, MO2:60ng). (C) Summary of rescue experiments. MO1 and MO2 were injected alone or with 2-6 ng GFP-MyoX mRNA at the 2-cell stage. At tadpole (St. 45) head width was measured as indicated in the examples shown. Red bars represent width distribution, percentages of embryos shown. Average head width increased with increasing doses of GFP-MyoX; mean values indicated by horizontal blue lines. At the 6 ng dose, the MO2 knockdown phenotype was rescued to nearly control levels. The MO1 rescue was significant but less complete. P values were determined using Student's T-test.

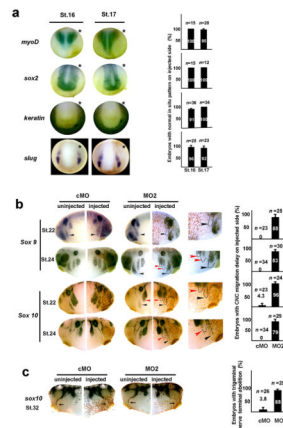


Figure 3. MyoX knockdown inhibited CNC migration and delays trigeminal nerve outgrowth (A) MyoX knockdown does not disrupt early induction of NC. Embryos were injected into one cell at the two-cell-stage with 30 ng MO2 and 5ng fluorescently-labeled control MO, cultured to stage 16/17, sorted using a fluorescent dissecting microscope to identify the injected side (on right in all cases shown, indicated by asterisks) and processed for whole-mount in situ hybridization with probes for mesoderm (*myoD*), neural plate (*sox2*), epidermis (*keratin*) and NC (*snail2*). No effect was observed. (B) MyoX knockdown inhibits cranial NC cell migration. Embryos unilaterally injected at two-cell stage with Control MO (cMO) or MO2, along with nuclear-localized lacZ RNA for lineage tracing, followed by Red-Gal staining (Research Organics), then whole mount in situ hybridization with *Sox9* and *Sox10* probes. St. 22; ventral migration of hyoid arch NC (black arrow head) and branchial arch NC (red arrow heads, dashed lines) was inhibited compared to the uninjected side (*Sox9*, 88%, n=25; *Sox10*, 96%, n=24.). The control MO had no effect. St.24; migration into all three arches occurred but was still retarded on the MO2-injected side (*Sox9*, 83%, n=30; *Sox10*, 79%, n=29). Enlarged views of the relevant regions from the MO2-injected side are shown to the right. (C) The trigeminal nerve was affected by loss of MyoX. Control MO or MO2 injected into one cell at the 2-cell stage. By St. 32, the distal region of the trigeminal nerve (arrows on the uninjected sides - left) was absent on the MO2-injected side (88%, n=25). The control MO (n=26) had no effect. Percentages and standard deviation error bars indicated to right as bar graphs.

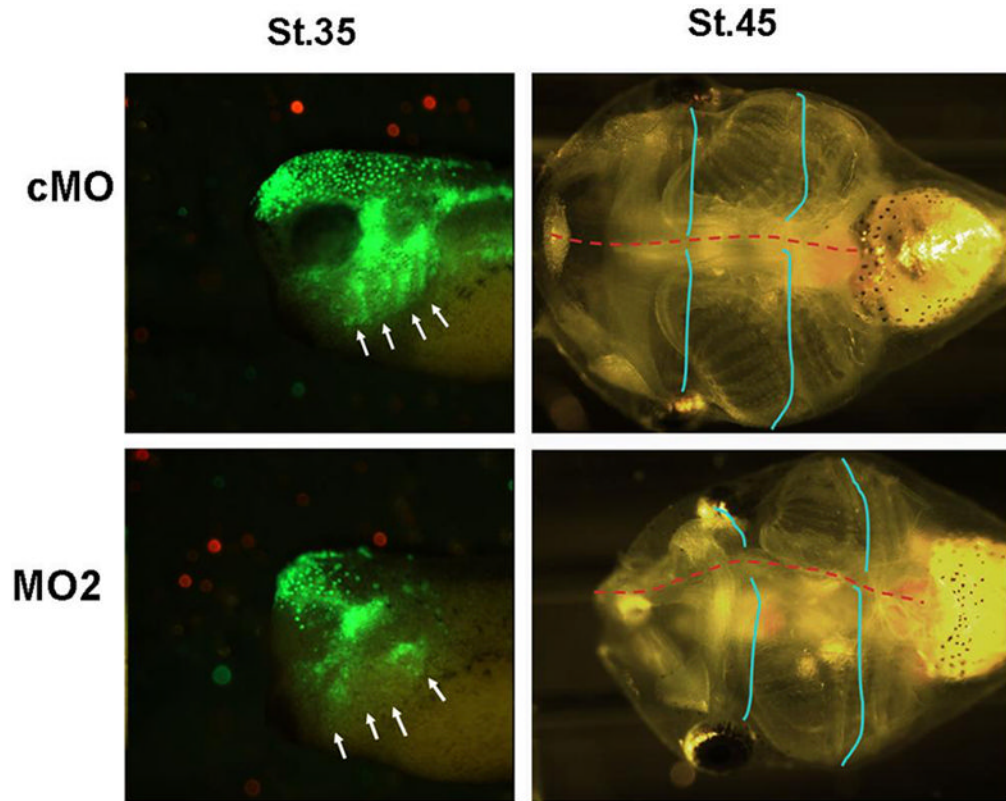


Figure 4. MyoX function in Cranial NC cell migration is cell-autonomous

Embryos were injected into one cell at the 16-cell (blastomere D1.2) or two cells at the 32-cell stage (blastomeres a2 and b2) with fluorescein dextran (15 ng/embryo; Invitrogen D-1821) plus control MO (2ng/embryo) or MO2 (2 ng/embryo). At early neurula (St. 13) correctly targeted embryos were identified using a fluorescence-equipped dissecting microscope. Donor CNC explants, including overlying ectoderm, were excised and transferred isotopically into stage-matched host embryos at St. 15. At St. 35, MO2 knockdown transplanted cells had migrated less extensively compared to controls (n=4/4), and exhibited cartilage deficiencies at tadpole stage. The control MO had no effect (n=4/4). Grafted sides are on top. Red dotted line: ventral middle line, Cyan line: length of ceratohyal or branchial cartilage. Arrows: branchial arches.

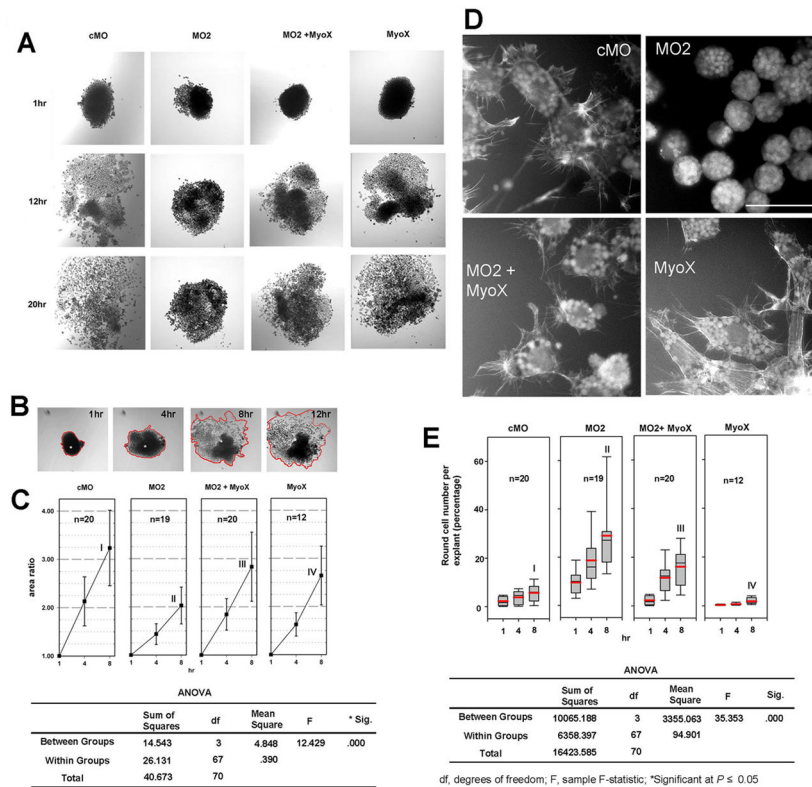


Figure 5. MyoX knockdown disrupts attachment, spreading and migration of CNC cells on fibronectin in vitro

(A) Control MO (30 ng/cell), and MO2 (30 ng/cell) alone or with myc-MyoX RNA (3 ng/cell) were injected into both cells of two-cell stage embryos. CNC explants were excised as described (Alfandari et al., 2003) and transferred to fibronectin-coated plates. Control cells attached and began to migrate within 20 min. Still images at 1, 12 and 25 hr shown. MO2 knockdown explants attached more slowly, and migration was significantly inhibited. To quantify migration, the outer boundary formed by the most extensively migrated cells was traced at 1, 4 and 8 hr (B). The ratios of the areas to the values at 1 hr are shown by the line plot (C). One-way ANOVA test was performed for 8hr data. Error bars represent standard deviation. (D) Phalloidin staining of CNC cells at 20hr post plating. MO2-knockdown cells were rounded with little actin organization this phenotype was rescued by myc-MyoX RNA. Scale bars: 30 μ m (E) Attachment of CNC cells was measured by counting round cells separated from the central cell mass at the same time point following plating as in (C). Box and whisker plots display mean values in red lines. Tables list ANOVA values; further statistical analysis summarized in Fig. S4.